

Crystallization in block copolymer melts: Small soft structures that template larger hard structures

J. Patrick A. Fairclough

Department of Chemistry, University of Sheffield, Sheffield S3 7HF, United Kingdom

Shao-Min Mai

Department of Chemistry, University of Manchester, Manchester M13 9PL, United Kingdom

Mark W. Matsen

Polymer Science Centre, University of Reading, Reading, RG6 6AF, United Kingdom

Wim Bras

Netherlands Organizations for Scientific Research, DUBBLE CRG, ESRF, F38043, Grenoble Cedex, France

Loic Messe and Simon C. Turner

Department of Chemistry, University of Sheffield, Sheffield S3 7HF, United Kingdom

Anthony J. Gleeson

CLRC Daresbury Laboratory, Warrington, WA4 4AD, United Kingdom

Colin Booth

Department of Chemistry, University of Manchester, Manchester M13 9PL, United Kingdom

Ian W. Hamley

School of Chemistry, University of Leeds, Leeds LS2 9JT, United Kingdom

Anthony J. Ryan^{a)}

Department of Chemistry, University of Sheffield, Sheffield S3 7HF, United Kingdom

(Received 5 October 2000; accepted 6 December 2000)

The crystallization of shear oriented oxyethylene/oxybutylene (E/B) diblock copolymers has been studied by simultaneous small and wide angle x-ray scattering. Crystallization of ordered melts can be accompanied by a change in length scale and retention of the melt orientation. Lamellar melts crystallize with an increase in length scale with multiply folded E blocks and the B blocks slightly stretched from their melt conformation. Crystallization from oriented gyroid melts leads to an increase in length scale with preferred melt directions being selected. The retention of layer planes on crystallization from an ordered melt is caused by the local stretching of chains and the locally one-dimensional structure, despite the relative strength of the structural process. We demonstrate that an interfacial preordering effect can cause crystallographic register to jump length scales in a soft matter system showing epitaxial crystallization. © 2001 American Institute of Physics. [DOI: 10.1063/1.1344605]

INTRODUCTION

Self-assembly of amphiphilic molecules provides one of the fundamental structure directing processes for building hierarchical structures in nature.¹ The universality of pattern formation by lipid membranes, lyotropic and thermotropic liquid crystals, and block copolymers,¹⁻³ all soft structures that are closely related to biological materials, is striking. Classical structures of lamellae, hexagonally ordered cylinders and cubic arrays of spheres are well established^{1,4} and it is easy to visualize how they act as templates. Complex cubic structures, such as the bicontinuous double diamond ($Pn\bar{3}m$) and gyroid ($Ia\bar{3}d$) have been found in lyotropic liquid crystals² and in block copolymer melts⁵⁻⁷ and solutions⁸ as well as in naturally occurring lipids,^{1,9,10} these also act as templates but in a more subtle manner. Here we report a transformation from a soft structure (block copoly-

mer melt) to a hard structure (semicrystalline block copolymer) with conservation of preferred lattice directions and a doubling of the lattice spacing.

How can one make a large hierarchical structure? Hard (crystalline) materials cannot form large scale structures directly but need soft materials, which have the ability to self-assemble, act as templates, and direct structure formation. Another important question is, what circumstances allow the retention of crystallographic register?—especially when the free energy changes associated with the two processes, templating and hard material growth, are quite different. Structures in lipids, liquid crystals, and block copolymers are typical of “soft” condensed matter where the material has a large scale structure with crystallographic register, but where the local atomic structure is liquidlike and disordered. These large scale structures are formed due to a balance of forces minimizing the Gibbs energy and are truly at dynamic equilibrium.¹⁰ In the case of block copolymers the important features are the configurational entropy of the molecules and

^{a)} Author to whom correspondence should be addressed; electronic mail: a.ryan@shef.ac.uk

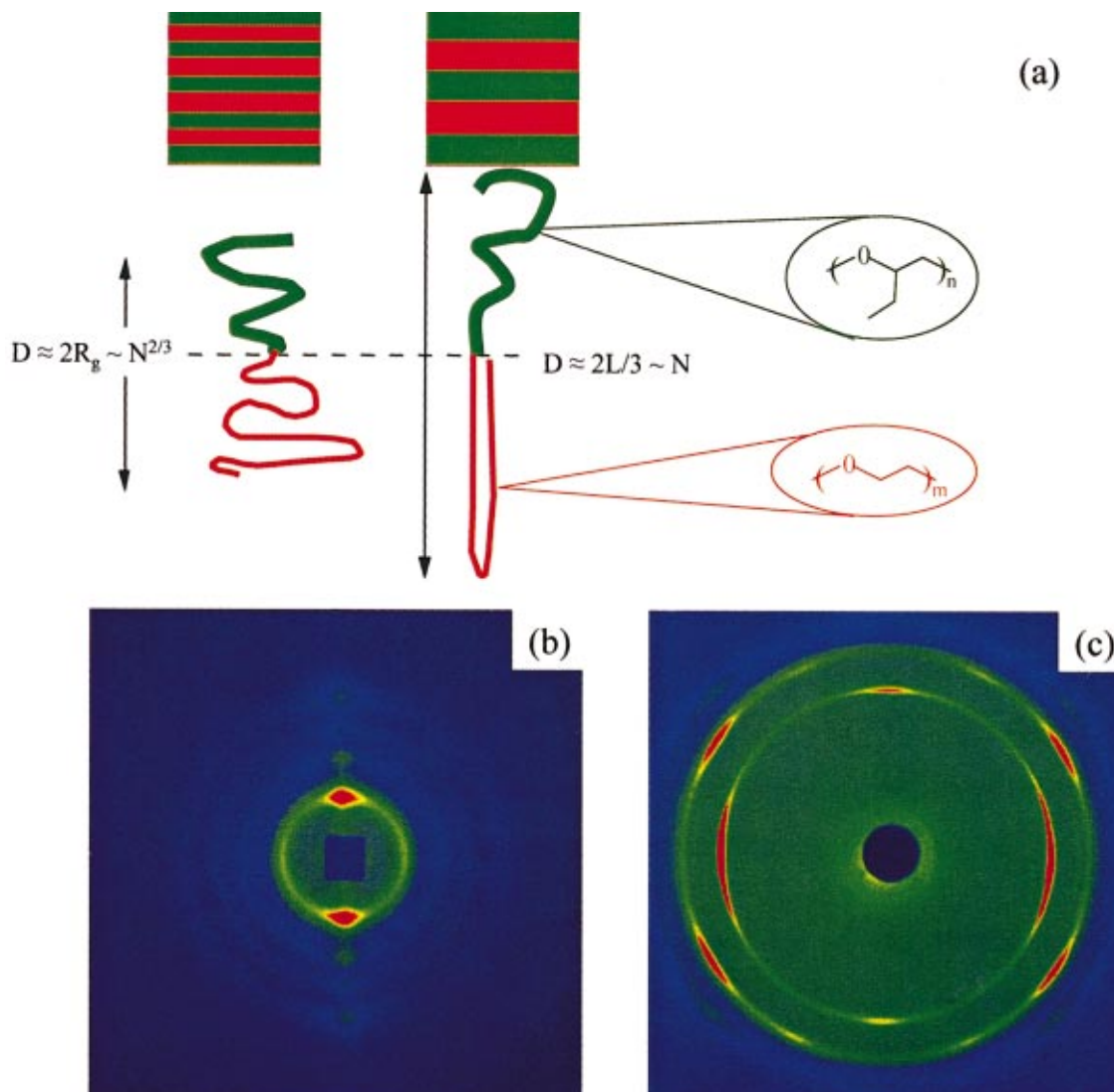


FIG. 1. (Color) (a) A schematic representation of block copolymer chain conformation in the molten and crystalline states. In the disordered melt the chains are Gaussian and have a size which scales as $N^{1/2}$, whereas in the ordered melt the chains are stretched from their Gaussian conformations and have a domain spacing which scales as $N^{2/3}$. When one of the blocks crystallizes into a straight stem the amorphous chains are stretched from their Gaussian conformations and have a domain spacing that scales as N . (b) Small angle x-ray scattering data from a sample of $E_{76}B_{38}$ that had been crystallized after shearing in the melt. It shows a pair of first-order reflections from the lamellar crystals with a d spacing of 224 Å. There are clearly resolved second-, third- and fourth-order reflections and the minimal arcing illustrates that the material is a monodomain with lamellae oriented in the shear direction. (c) Wide angle x-ray diffraction data from a sample of $E_{76}B_{38}$ that had been crystallized after shearing in the melt. Fiber diffraction of poly(oxyethylene) (Ref. 22) shows that the E chains are oriented perpendicular to the lamellar interfaces as the strong equatorial reflection is the c axis (001 reflection) of the unit cell.

the formation of interfacial area. The theory, which describes these phenomena, is well developed¹¹ and gives accurate predictions of phase behavior. The gyroid ($Ia\bar{3}d$) phase has been observed between the lamellar and hexagonal packed cylinder phases in the diblock copolymer phase diagram close to the order-disorder transition;^{6,12} it comprises cylindrical channels of the minority material joined by threefold connectors, two such lattices with opposite chirality interpenetrate through a matrix.

One important class of structure direction is soft-soft templating between mesoscopic structures. Transformations between adjacent gyroid and lamellar or hexagonal phases have attracted attention because they are related to the structural transitions which occur when cells fuse or rupture. A number of studies of anionic and nonionic surfactants have provided evidence of epitaxial relationships in transforma-

tions of gyroid to lamellar^{13,14} with growth proceeding along [111] directions without change in lattice parameters. This is thought to be related to the orientation of the threefold connectors within the unit cell. A similar epitaxial relationship has been observed for a diblock copolymer melt¹⁵ where the lamellar phase grows from the gyroid without long-range transport of material and with preservation of orientation in some layer planes. In these epitaxial transformations the lattice spacing is either conserved or changes smoothly as the high-symmetry cubic structure transforms into the lower symmetry layered or rodlike structure. This is usual in structural transformation in both soft and hard-condensed matter. Soft-hard templating, by block copolymers and surfactants, of porous and composite structure on the nanometer scale has provoked much interest for formation of mesostructured inorganic^{16,17} and organic materials.¹⁸ In these cases there is

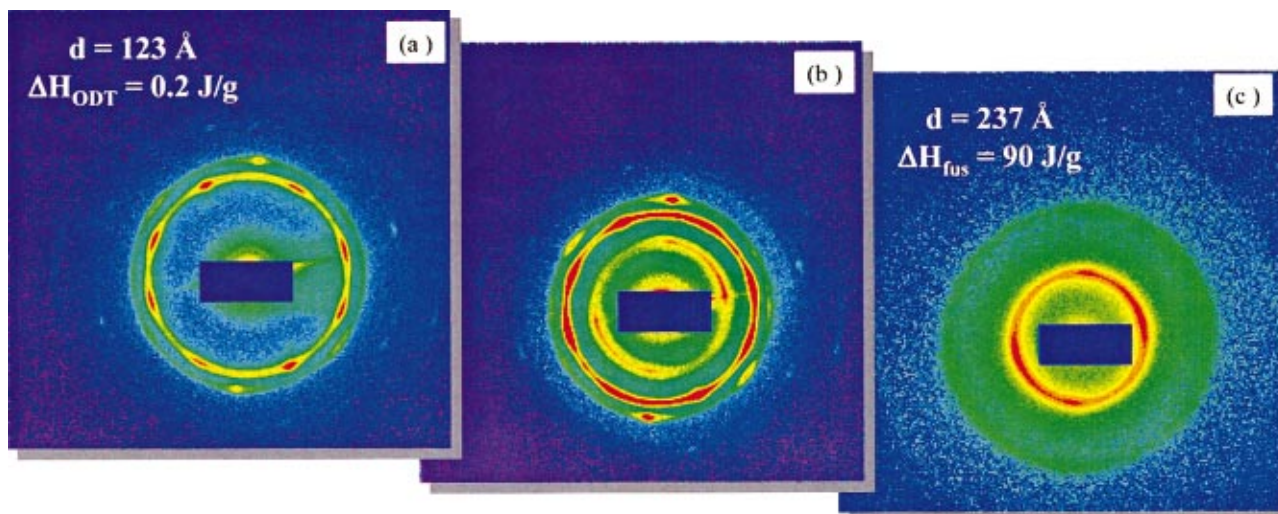


FIG. 2. (Color) A series of SAXS patterns showing the transformation of a bicontinuous ($Ia\bar{3}d$) cubic melt of $E_{75}B_{54}$ into an oriented lamellar crystal. (a) The (inner) 10 spot pattern is from a two-dimensional powder made up of grains rotated randomly around the $[111]$ lattice direction which has become preferentially oriented parallel to the shear. (b) Once crystallization starts strong scattering is observed inside the $\langle 211 \rangle$ reflections of the melt. Lamellar crystals, nucleated from the cubic melt, are observed to grow in a number of preferred directions, corresponding to the $\langle 211 \rangle$ and $\langle 220 \rangle$ reflections of the $Ia\bar{3}d$. These lamellar crystals are consuming the ordered melt and the higher orders of the $Ia\bar{3}d$ are still clearly visible. (c) Eventually the $Ia\bar{3}d$ melt is nearly all consumed and higher order reflections can be seen for the lamellar crystals. There has been a transformation along the two crystallographic planes of the $Ia\bar{3}d$ cubic structure with d spacing 123 ± 2 Å to an oriented lamellar structure with d spacing 237 ± 5 Å.

no crystallographic register between the soft template and the growing hard phase and structural transformations are observed as chemical reactions change the thermodynamic interactions between components.¹⁸ However if epitaxy is observed then there is nearly always a continuous change in lattice parameters.

EXPERIMENT

The amphiphilic system reported here has been extensively studied including self-assembly in dilute and concen-

trated aqueous solutions,¹⁹ microphase separation in the melt²⁰ and crystallization behavior.²¹ Block copolymers with narrow molecular weight distributions were prepared by sequential anionic polymerization of ethylene oxide (E) followed by 1,2-butylene oxide (B). Vacuum line and ampoule techniques were used throughout and the copolymers were characterized by gel permeation chromatography and ¹³C nuclear magnetic resonance spectroscopy. The molecular characteristics are expressed in E_mB_n notation where the subscripts denote the average numbers of repeat units.

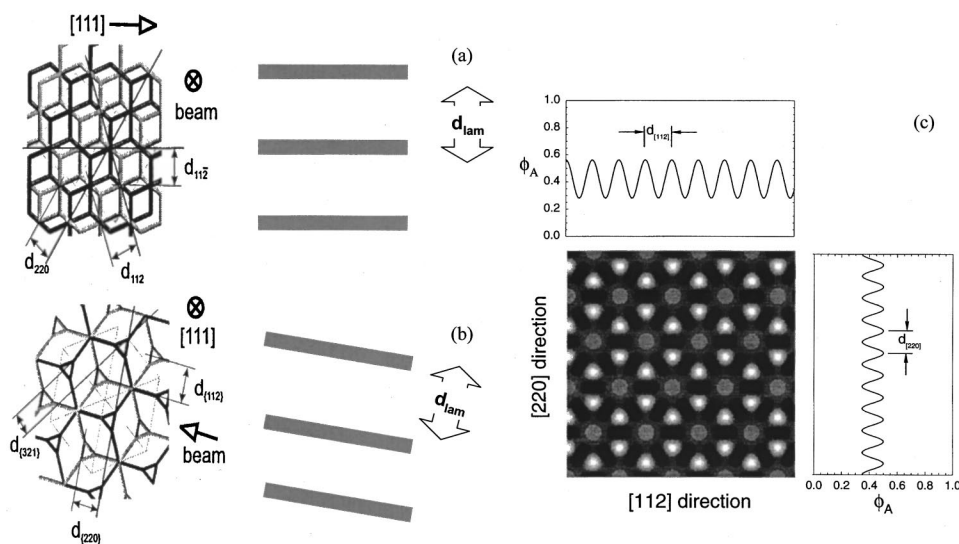


FIG. 3. Schematics of the $Ia\bar{3}d$ morphology showing the orientation of the three-functional connectors and the principal crystallographic directions. (a) A two-dimensional projection (Ref. 15) that shows the formation of aligned lamellae by crystallization along every second $\langle 112 \rangle$ plane. (b) A view along the $[111]$ direction (Ref. 15) displaying $\{211\}$, $\{220\}$, and $\{321\}$ planes which transform into aligned lamellae by crystallization along every second $\langle 211 \rangle$ plane. (c) A two-dimensional image of composition, $\Phi_A(r)$, averaged in the $[111]$ direction with the corresponding one-dimensional (1D) plots resulting from the average of Φ_A in the $[112]$ and $[220]$ directions. This establishes that the gyroid phase is most lamellarlike in the $[112]$ direction because the uppermost 1D plot has the strongest oscillation.

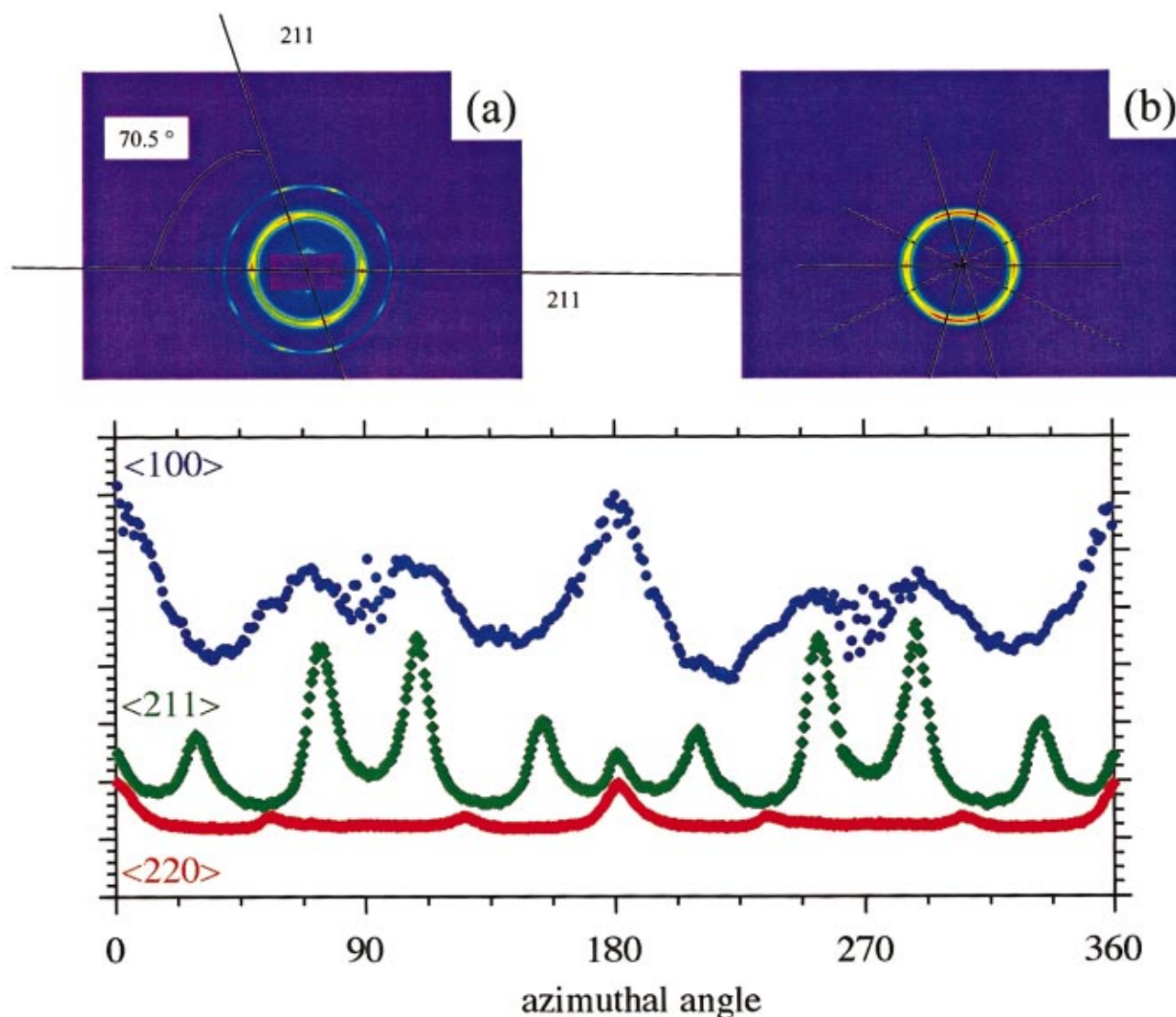


FIG. 4. (Color) The relationship between the gyroid melt structure and the semicrystalline structure of $E_{75}B_{54}$. (a) Superimposition of the SAXS patterns from the $Ia\bar{3}d$ melt and fully crystalline sample showing that the two lamellar orientations observed are consistent with the $\langle 112 \rangle$ and $\langle 1\bar{1}2 \rangle$ reflections. The lamellar reflections are separated by 70.5° as expected for $Ia\bar{3}d$ (Ref. 15). The scattering measurements are made on a small scattering volume of 0.125 mm^3 and sample only a small number of grains. (b) Scattering from the same fully crystalline sample with a much larger scattering volume of 2.5 mm^3 . The solid lines show the $\langle 211 \rangle$ reflections that are followed by crystallization, the dotted lines those not so obviously sampled. It should be noted that the peaks in the crystalline sample are superimposed on a bright ring implying some loss of overall orientation. (c) Azimuthal scans (with respect to the meridional direction) showing the relative intensities of the $\langle 211 \rangle$ and $\langle 220 \rangle$ in the melt compared to the crystalline lamellae $\langle 100 \rangle$ peaks in the solid.

Simultaneous small/wide angle x-ray scattering (SAXS/WAXS) measurements were made on beamline 16.1 at the Daresbury Synchrotron Radiation Source or on the DUBBLE beamline at the European Synchrotron Radiation Source (ESRF). At Daresbury the incident beam was 1.4 \AA and a Fuji image plate at 10 cm was used to record the WAXS pattern with a 10 mm hole to allow the SAXS pattern to develop out at 3 m for recording on an area detector. At the ESRF the incident beam was 1.0 \AA and an area detector was used to record the SAXS at 4 m. The sample thickness was 1 mm and the beam passed through a hole of 3 mm which was covered with KaptonTM tape. The sample was oriented by shearing the ordered melt, for 50 cycles at approximately 1 Hz and 200% strain, in a heated cell consisting of a piece of brass with machined side grooves to allow movement of a

parallel brass slider during shear, the polymer temperature was monitored by a thermocouple. Quiescent cooling after shear orientation allowed the epitaxial relationships to be observed.

RESULTS AND DISCUSSION

The crystallization of melts of E_mB_n copolymers has been studied in some detail²¹ and the orientation of the crystal stems perpendicular to lamellar interfaces is well established. This is soft-hard templating but with obvious epitaxial relationships. The simplest case of a copolymer with a lamellar melt phase and a lamellar semicrystalline phase is illustrated in Fig. 1(a) by a schematic of the molecular conformations of $E_{76}B_{38}$ in the equilibrium melt and crystallized

states. In the melt the characteristic length scale, D , is that of the stretched coil with a length dependent on the radius of gyration, R_g , whereas in the crystalline state the characteristic length scale is related to the extended chain length, L . The low temperature structure is a once-folded E block (two crystal stems) and an unfolded, stretched B block: An unfolded E chain would not be possible due to conservation of volume. The SAXS pattern in Fig. 1(b) is obtained from a sample of $E_{76}B_{38}$ that was shear oriented prior to crystallization. It shows first-order reflections from the lamellar crystals with a d spacing of 224 Å. There are clearly resolved second-, third-, and fourth-order reflections and the minimal arcing illustrates that the material is a monodomain with lamellas oriented in the shear direction. The simultaneously recorded WAXS pattern in Fig. 1(c) confirms that the E chains are oriented perpendicular to the lamellar interfaces, the strong equatorial reflections derived from the c axis $\{001\}$ of the helical E block.²² SAXS²¹ shows a change in length scale from 109 Å in the ordered melt to 224 Å in the crystal phase, i.e., there is a step change in lattice spacing on transformation from the soft ordered melt structure to the hard semicrystalline solid structure with an approximate doubling of lattice spacing due to stretching of chains perpendicular to the lamellar interface with corresponding lateral contraction.

The terms “soft” and “hard,” as applied here to the ordered melt and semicrystalline solid, are justified by the enthalpy of formation of the structures and the mechanical properties of the materials. High resolution calorimetry²³ studies on $E_{60}B_{29}$ show that the latent heat of the fusion process is $90.2 \pm 2 \text{ J g}^{-1}$ whereas that of the order-disorder transition in the melt is $0.171 \pm 0.003 \text{ J g}^{-1}$. The enthalpy of formation of crystals is 500 times larger than that of the ordered melt. Similarly the shear modulus of the semicrystalline polymer is 10^7 Pa whereas that of the ordered melt is 10^5 Pa .

Ordered block copolymer melts have chains that are stretched compared to the random (Gaussian) conformations.^{3,11} The characteristic length of a strongly segregated melt scales with $N^{2/3}$ compared with $N^{1/2}$ for a Gaussian chain. Furthermore, the stretching is not uniform, chain segments are more strongly oriented across the interface between the two chain types. It is feasible that it is the local orientation of chain segments perpendicular to the interfaces that nucleates crystallization. The local orientation reduces the crystallization energy barrier (crystallization in polymers requires development of orientational order along the chain) and promotes crystal growth. For this reason the vast majority of semicrystalline block copolymers show stems perpendicular to lamellar surfaces. The conditions for formation of other orientations and morphologies must be strongly forcing, i.e., confinement of the crystallizing chains by hard walls^{24,25} and with chain imperfections that prevent formation of large crystals.

The retention of orientation of layer planes on crystallization from a lamellar ordered melt is not unexpected given the local stretching of chains and the one-dimensional structure, despite the strong driving force for the transition. What is unexpected, however, is that a more complex soft structure will also direct crystallization processes. The SAXS patterns

in Fig. 2 follow the transformation of a gyroid melt into a lamellar crystal. The SAXS pattern in Fig. 2(a) was obtained following large amplitude oscillatory shear and is typical^{6,12,15} of the gyroid morphology. The ten-spot pattern is from directionally oriented $Ia\bar{3}d$ crystals with the zone axis along the $[111]$ lattice direction which is oriented parallel to the shear direction.^{15,26} This oriented melt structure was allowed to cool from 80 to 20 °C over a period of an hour. Orientation was maintained after shearing and many higher order reflections were sampled. Once crystallization starts strong scattering was observed inside the $\langle 211 \rangle$ reflections of the melt. The example shown in Fig. 2(b) shows simultaneous growth in two of the $\{211\}$ planes. Repeated experiments (at Daresbury and the ESRF) showed crystal growth to be observed preferentially in three of the five $\{211\}$ planes. These lamellar crystals are consuming the ordered melt the presence of which is confirmed since the higher orders of $Ia\bar{3}d$ are still clearly visible. Eventually [Fig. 2(c)] the gyroid melt is nearly all consumed and higher order reflections can be seen for the lamellar crystals. There has been a transformation in two of the $\{211\}$ planes of the $Ia\bar{3}d$ cubic structure with d spacing $123 \pm 2 \text{ Å}$ to an oriented lamellar structure with d spacing $237 \pm 5 \text{ Å}$. If there is epitaxy from the $Ia\bar{3}d$ to the lamellar structure then there are 24 equivalent planes available. In this experiment we have Bragg sampled two of these planes during the crystallization of a $\{111\}$ zone oriented crystal of $Ia\bar{3}d$ melt.

In the gyroid morphology, chain stretching is uniform (within 7%)²⁶ across the interface between microphases and consequently crystallization can nucleate anywhere around this surface. The absolute magnitude of the change in characteristic length on crystallization is determined by the crystallization temperature and block lengths, in the example given here the length scale doubles. The effective doubling of the plane separation is illustrated in Fig. 3(a) and 3(b) where unit cells are shown transforming along $\{111\}$ into two lamellar unit cells. Fig. 3(c) shows average segmental density profiles across the $[112]$ and $[220]$ directions of the gyroid phase, calculated using self-consistent field methods,^{4,11,26} and the density map of the structure as it would appear in the transmission electron microscope looking down the $\{111\}$ axis. These calculations provide strong evidence that lamellae orient along $[211]$ directions because that is the direction in which the gyroid phase most resembles a lamellar phase.

The stretching is localized to the interface and this is where we would expect crystallization to initiate. Statistically crystals that initiate are likely to grow fastest in the direction most able to provide room for growth, i.e., the most lamellarlike directions. Consequently, the crystallization follows the lamellarlike direction initially and then breaks out to a longer length scale. The initial crystallization is the symmetry breaking step and retains the preferred direction of the soft cubic structure even though the length scale increases. Once a sample has been crystallized and the gyroid symmetry broken, remelting results in an unoriented melt structure with a powder pattern. Recent experimental and theoretical²⁷ work on polymer crystallization has shown that the local

TABLE I. The predicted relative intensities from a gyroid melt randomly oriented about the [111] direction compared to those observed in the azimuthal intensity measurements.

Observed intensity	$\langle 211 \rangle$ Azimuthal position/(°)	Predicted intensity
1	0, 180	1
1.3	28.1, 151.9, 208.1, 311.9	1.14
3.2	70.5, 109.5, 250.5, 289.5	1.50
Observed intensity	$\langle 220 \rangle$ Azimuthal position	Predicted intensity
3.2	0, 180	1.15
1	54.7, 125.3, 234.7, 305.3	1

structure of the polymer melt, prior to crystallization, has a strong influence on the nature of the crystallization process. The local orientation at the block copolymer interfaces reduces the crystallization energy barrier causing the epitaxial relationships observed.

In Fig. 4 we compare the scattering pattern from the melt and the crystals to confirm the epitaxial relationships. In Fig. 4(a) the melt and crystal structures from a small scattering volume (0.125 mm^3) clearly illustrate that the crystallization selects the specific (211) planes and the lamellar peaks lie on these planes separated by 70.5° . We suspect that there are two domains in the Bragg condition giving rise to these two sets of lamellar reflections and this gives indirect evidence of the grain size. In Fig. 4(b), however, there is a much larger scattering volume (2.5 mm^3) and more lamellar domains are sampled. Now three of the five $\{211\}$ planes are obviously preferred and these are highlighted by the solid lines in Fig. 4(b) and by the azimuthal intensity scans in Fig. 4(c). In repeated crystallization we do not observe strong crystalline reflections in the directions highlighted by the dotted lines.

The $Ia\bar{3}d$ structure obtained by large amplitude oscillatory shear is a highly twinned body centered cubic structure with a [111] direction along the shear direction,¹⁵ the intensities predicted for the $\langle 211 \rangle$ and $\langle 220 \rangle$ reflections are given in Table I. There are eight orientations of grains with a common [111] zone axis that are sampled to make up the observed pattern. The $\langle 211 \rangle$ reflections at 70.5° , 109.5° , 205.5° , and 289.5° and the $\langle 220 \rangle$ reflections at 0° and 180° come from the two projections of the unit cell with the $\{111\}$ planes parallel to the shear direction and the $\{220\}$ planes along the shear gradient, i.e., perpendicular to the shear plates and the x-ray beam. The shear conditions used have obviously caused preferential orientation about this direction and this is seen by the fact that these reflections are at least twice as strong as predicted (see Table I). Furthermore the samples were cooled slowly after shear orientation so the $[220]$ direction is also preferentially aligned along the thermal gradient during crystallization. We conclude that the sample crystallizes most rapidly along a $[211]$ direction in grains which are oriented with their $\langle 220 \rangle$ directions parallel to the shear and thermal gradient. Furthermore grains with this orientation in the melt are observed to be in the Bragg conditions at least twice as frequently than in a randomly rotated set of grains. Crystallization could select these grains to crystallize in the thermal gradient direction, consuming

the other adjacent orientations. The SAXS patterns in Fig. 4(a) indicate that the grains are of the order of $10 \mu\text{m}$ in size and only two orientations (and possibly tens of grains) are sampled in Fig. 4(a). In contrast there are many grains sampled in Fig. 4(b) where there are oriented peaks on a strong lamellar ring.

SUMMARY AND CONCLUSIONS

We have demonstrated here that an interfacial preordering effect can cause crystallographic register to jump length scales in soft–hard templating. The retention of layer planes on crystallization from an ordered melt is caused by the local stretching of chains and the locally one-dimensional structure, despite the relative strengths of the structural process. What is unexpected, however, is that a complex soft structure will also direct the crystallization processes, selecting specific orientations. We have considered many options for this, including low-angle grain boundaries, but conclude that there is a subtlety in the local chain orientation that provides the selection process. Small soft structures (lipid membranes) directing larger hierarchical structures (bone and exoskeleton) are common in natural systems. We present here a soft matter system showing epitaxial crystallization and length-scale jumping.

¹P. Ball, *The Self-Made Tapestry* (Oxford University Press, Oxford, 1998).

²J. M. Seddon, *Biochim. Biophys. Acta* **1**, 1031 (1990).

³I. W. Hamley, *The Physics of Block Copolymers* (Oxford University Press, Oxford, 1998).

⁴F. S. Bates and G. H. Fredrickson, *Annu. Rev. Mater. Sci.* **26**, 501 (1996).

⁵E. L. Thomas and R. L. Lascanec, *Philos. Trans. R. Soc. London, Ser. A* **348**, 149 (1994).

⁶S. Förster, A. K. Khandpur, J. Zhao, F. S. Bates, I. W. Hamley, A. J. Ryan, and W. Bras, *Macromolecules* **27**, 6922 (1994).

⁷E. L. Thomas, D. M. Anderson, C. S. Henkee, and D. Hoffman, *Nature (London)* **334**, 598 (1988).

⁸D. A. Hajduk, M. B. Kossuth, M. A. Hillmyer, and F. S. Bates, *J. Phys. Chem. B* **102**, 4269 (1998).

⁹M. Clerc, P. Laggner, A.-M. Levelut, and G. Rapp, *J. Phys. II* **5**, 901 (1995).

¹⁰V. Luzzatti, *Nature (London)* **218**, 1031 (1968).

¹¹M. W. Matsen and F. S. Bates, *Macromolecules* **29**, 1091 (1996).

¹²D. A. Hajduk, P. E. Harper, S. M. Gruner, C. C. Honeker, G. Kim, E. L. Thomas, and L. J. Fetters, *Macromolecules* **27**, 4063 (1994).

¹³Y. Rancan and J. Charvolin, *J. Phys. Chem.* **92**, 2646 (1988).

¹⁴P. Kekicheff and B. Cabane, *Acta Crystallogr., Sect. B: Struct. Sci.* **44**, 395 (1988).

¹⁵M. E. Vigild, K. Almdal, K. Mortensen, I. W. Hamley, J. P. A. Fairclough, and A. J. Ryan, *Macromolecules* **31**, 5702 (1998).

¹⁶A. Firouzi, D. Kumar, L. M. Bull, T. Besier, P. Sieger, Q. Huo, S. A. Walker, J. A. Zasadzinski, and C. Glinka, *Science* **267**, 1138 (1995).

¹⁷D. Y. Zhao, J. L. Feng, Q. S. Huo, N. Melosh, G. H. Fredrickson, B. F. Chmelka, and G. D. Stucky, *Science* **279**, 548 (1998).

¹⁸P. M. Lipic, F. S. Bates, and M. A. Hillmyer, *J. Am. Chem. Soc.* **120**, 8963 (1998).

¹⁹A. Kellarakis, W. Mingvanish, C. Daniel, H. Li, V. Havredaki, C. Booth, I. W. Hamley, and A. J. Ryan, *Phys. Chem. Chem. Phys.* **2**, 2755 (2000).

²⁰S.-M. Mai, J. P. A. Fairclough, N. J. Terrill, S. Turner, I. W. Hamley, M. W. Matsen, A. J. Ryan, and C. Booth, *Macromolecules* **31**, 8110 (1998).

²¹S. M. Mai, J. P. A. Fairclough, K. Viras, P. A. Gorry, I. W. Hamley, A. J. Ryan, and C. Booth, *Macromolecules* **30**, 8392 (1997).

²²Y. Takahashi, and H. Tadokoro, *Macromolecules* **6**, 672 (1973).

- ²³V. P. Voronov, V. M. Buleikov, V. E. Podneks, I. W. Hamley, J. P. A. Fairclough, A. J. Ryan, S.-M. Mai, B.-X. Liao, and C. Booth, *Macromolecules* **30**, 6674 (1997).
- ²⁴I. W. Hamley, J. P. Fairclough, N. J. Terrill, A. J. Ryan, P. Lipic, F. S. Bates, and E. Towns-Andrews, *Macromolecules* **29**, 8835 (1996).
- ²⁵D. J. Quiram, R. A. Register, G. R. Marchand, and D. H. Adamson, *Macromolecules* **31**, 4891 (1998).
- ²⁶M. W. Matsen, and F. S. Bates, *Macromolecules* **29**, 7641 (1996).
- ²⁷P. D. Olmsted, W. C. K. Poon, T. C. B. McLeish, N. J. Terrill, and A. J. Ryan, *Phys. Rev. Lett.* **81**, 373 (1998).